LIMITS ON VERY HIGH ENERGY EMISSION FROM GAMMA-RAY BURSTS WITH THE MILAGRO OBSERVATORY

R. ATKINS,[1] W. BENBOW,[2,3] D. BERLEY,[4] E. BLAUFUSS,[4] J. BUSSONS,[4,5] D. G. COYNE,[2] T. DEYOUNG,[2,4] B. L. DINGUS,[6]
D. E. DORFAN,[2] R. W. ELLSWORTH,[7] L. FLEYSHER,[8] R. FLEYSHER,[8] G. GISLER,[6] M. M. GONZALEZ,[1] J. A. GOODMAN,[4]
T. J. HAINES,[6] E. HAYS,[4] C. M. HOFFMAN,[6] L. A. KELLEY,[2] J. E. MCENERY,[1,9] R. S. MILLER,[10] A. I. MINCER,[8]
M. F. MORALES,[2,11,12] P. NEMETHY,[8] D. NOYES,[4] J. M. RYAN,[10] F. W. SAMUELSON,[6] A. SHOUP,[13] G. SINNIS,[6]
A. J. SMITH,[4] G. W. SULLIVAN,[4] D. A. WILLIAMS,[2] S. WESTERHOFF,[2,14]
M. E. WILSON,[1] X. XU,[6] AND G. B. YODH[13]

ABSTRACT

The Milagro telescope monitors the northern sky for 100 GeV–100 TeV transient emission through continuous very high energy (VHE) wide-field observations. The large effective area and ∼100 GeV energy threshold of Milagro allow it to detect VHE gamma-ray burst (GRB) emission with much higher sensitivity than previous instruments and a fluence sensitivity at VHE energies comparable to that of dedicated GRB satellites at keV–MeV energies. Even in the absence of a positive detection, VHE observations can place important constraints on GRB progenitor and emission models. We present limits on the VHE flux of 40 s–3 hr duration transients near Earth as well as sensitivity distributions that have been corrected for gamma-ray absorption by extragalactic background light and cosmological effects. The sensitivity distributions suggest that the typical intrinsic VHE fluence of GRBs is similar to or weaker than the keV–MeV emission, and we demonstrate how these sensitivity distributions may be used to place observational constraints on the absolute VHE luminosity of GRBs for any GRB emission and progenitor model.

Subject headings: gamma rays: bursts — gamma rays: observations

1. INTRODUCTION

Very high energy (VHE) gamma-ray burst (GRB) observations have the potential to constrain theoretical models of both the prompt and extended phases of GRB emission. Models based on both internal and external shocks have predicted VHE fluence comparable to, or in certain situations stronger than, the keV–MeV radiation, with durations ranging from shorter than the keV–MeV burst to extended TeV afterglows (Dermer & Chiang 2000; Pilla & Loeb 1998; Zhang & Mészáros 2001). GRB emission above 100 GeV is particularly sensitive to the Lorentz factor and the photon density of the emitting material— and thus the distance of the radiating shock from the source— owing to $\gamma\gamma \rightarrow e^+e^-$ absorption in the emission region.

EGRET observed several GRBs at GeV energies and observed no evidence of a high-energy rollover in the GRB spectrum

(Dingus 1995), and recent results by Gonzalez et al. (2003) indicate that the spectrum of some GRBs contains a very hard, luminous, long-duration component. At energies above a few hundred GeV, several observation attempts have been made, including coincidence observations between the Tibet air shower array and BATSE (Amenomori et al. 1996), rapid follow-up observations by the Whipple Air Cerenkov telescope (Connaughton et al. 1997), and coincident and monitoring studies by AIROBICC (Padilla et al. 1998), Whipple (Connaughton et al. 1998), and the Milagro prototype (Atkins et al. 2000a; Leonor 2000; McCullough 2001). While several of these studies have reported evidence for VHE GRB emission, no clear picture of the VHE emission from GRBs has emerged.

In recent years, the rate of possible GRB coincident detections has been relatively low owing to the absence of sensitive, large field of view GRB detectors like BATSE. However, Milagro is a very sensitive detector with a low ∼100 GeV energy threshold and wide ≳2 sr field of view and is fully capable of autonomous identification of a VHE burst of emission. The low-energy threshold is particularly important because of the reduced attenuation by extragalactic background light near 100 GeV (Jelley 1966; Primack et al. 1999; Stecker & de Jager 1998), which dramatically increases the volume of space observed. This Letter details the monitoring of the northern sky for VHE transients of 40 s–3 hr duration with the Milagro observatory.

2. THE 40 s–3 hr TRANSIENT SEARCH IN MILAGRO

VHE gamma rays incident on the Earth interact in the upper atmosphere and produce extensive air showers (EASs) that propagate to lower altitudes. Milagro uses the water Cerenkov technique to detect EASs by converting the wave front of relativistic particles in the EASs into a front of Cerenkov light, detected by photomultiplier tubes (PMTs; Atkins et al. 2000b). The amplitude and arrival time of the PMT signals are analyzed to determine the direction and characteristics of the ∼1800 EASs per second detected by Milagro, most of which are

[1] Department of Physics, University of Wisconsin–Madison, 1150 University Avenue, Madison, WI 53706.

[2] Santa Cruz Institute for Particle Physics, University of California at Santa Cruz, 1156 High Street, Santa Cruz, CA 95064.

[3] Current address: Max-Planck-Institut für Kernphysik, Postfach 103980, D-69029, Heidelberg, Germany.

[4] Department of Physics, University of Maryland, College Park, MD 20742.

[5] Current address: Université de Montpellier II, Montpellier Cedex 5, F-34095, France.

[6] Los Alamos National Laboratory, P.O. Box 1663, Los Alamos, NM 87545.

[7] Department of Physics and Astronomy, George Mason University, 4400 University Drive, Fairfax, VA 22030.

[8] Department of Physics, New York University, 4 Washington Place, New York, NY 10003.

[9] Current address: NASA Goddard Space Flight Center, Greenbelt, MD 20771.

[10] Department of Physics, University of New Hampshire, Demerrit Hall, Durham, NH 03824-3525.

[11] Current address: Massachusetts Institute of Technology, Center for Space Research, Building 37-664H, 77 Massachusetts Avenue, Cambridge, MA 02139.

[12] Corresponding author: (617) 452-3159; mmorales@space.mit.edu.

[13] Department of Physics and Astronomy, University of California, Irvine, CA 94697.

[14] Current address: Department of Physics, Columbia University, 538 West 120th Street, New York, NY 10027.

<div align="center">

TABLE 1

PROBABILITY OF GRB DETECTION BY MILAGRO

</div>

SEARCH INTERVAL (s)	TOTAL OBSERVATION DURATION (days)	L_{50} z			L_{51} z			L_{52} z		
		0–0.1	0.1–0.2	0.2–0.3	0–0.15	0.15–0.3	0.3–0.45	0–0.23	0.23–0.47	0.47–0.7
40	290.2	0.90	0.37	0.01	1.00	0.44	0.03	1.00	0.37	0.003
80	290.2	1.00	0.27	0.01	1.00	0.36	0.09	1.00	0.54	0.08
160	290.0	1.00	0.38	0.04	1.00	0.59	0.11	1.00	0.58	0.10
		z			z			z		
		0–0.15	0.15–0.3	0.3–0.45	0–0.23	0.23–0.47	0.47–0.7	0–0.23	0.23–0.47	0.47–0.7
320	289.7	0.73	0.10	0.00	1.00	0.18	0.01	1.00	0.68	0.17
640	289.2	0.91	0.20	0.01	1.00	0.27	0.01	1.00	0.81	0.24
1280	288.1	1.00	0.28	0.02	1.00	0.31	0.03	1.00	...	...
2560	286.1	1.00	0.45	0.03	1.00	0.40	0.07	1.00	...	...
5120	282.2	1.00	0.47	0.05	1.00	0.48	0.08	1.00	...	...
10240	275.7	1.00	0.51	0.13	1.00	0.54	0.13	1.00	...	...

NOTES.—This table indicates the probability of a GRB of given duration, absolute luminosity, and redshift within the 1.84 sr field of view of this analysis being detected by the Milagro experiment. L_x indicates the absolute luminosity (not corrected for beaming) in units of 10^x ergs s^{-1} between 100 GeV and 21 TeV. Since the SFR and space volume both increase with redshift, the median redshift of the events used to calculate each probability is not in the center their redshift bin but instead much nearer to the upper redshift value. The ellipses represent values that were not calculated owing to computational constraints.

initiated by cosmic-ray nuclei. The water Cerenkov technique enables Milagro to operate continuously.

The precision of the Milagro event reconstruction depends strongly on the shower characteristics, leading to a point-spread function (PSF) for the initiating particle direction which varies considerably from event to event. The arrival times measured by the PMTs are fitted to a plane, after making corrections based on the pulse amplitude in each PMT and the distance of the PMT from the reconstructed shower core. The shower fit proceeds through several iterations, at each stage removing times with large residuals to the fitted shower plane. Showers reconstructed within 45° of zenith are kept for further analysis. The number of PMT times surviving in the final iteration is called n_{fit}, which is used in conjunction with the reduced χ^2 to characterize the quality of the reconstruction. The showers are then separated into 13 classes, based on the values of n_{fit} and χ^2, such that events within each class have similar angular PSFs (see Morales 2002 for details). In general, the width of the PSF decreases as n_{fit} increases or χ^2 decreases. The class with the worst PSF is removed from further analysis, at a negligible cost in sensitivity, because the PSF is so broad that it could not be readily handled by the code used to accumulate the sky maps.

The characteristics of the light recorded by PMTs at the bottom of the reservoir can be used to reject background cosmic-ray showers in favor of gamma rays using a quantity we call "compactness" (Atkins et al. 2003). Events are assigned a weight, between 0 and 1, based on the relative probability of the event being a background cosmic ray or a gamma ray, given the compactness value and to which of the 12 remaining PSF classes the event belongs. To speed the computation, events with weight less than 0.5 are rejected.

This search implements an analysis method developed by Morales, Williams, & DeYoung (2004), which efficiently includes the event-by-event PSF and photon probability (i.e., background rejection) information, enhancing the sensitivity of the observations. The technique uses the characteristics described above to determine a spatial photon probability density—the expected PSF of the event multiplied by the probability the shower was initiated by a gamma ray—which is then added to a sky map to form the estimated total photon density. Therefore, rather than considering each photon as a point at

each reconstructed event location, the new technique instead places a smooth distribution at that location, with the shape of the distribution mirroring the reconstruction accuracy of the detector. The probability of the background, which primarily consists of cosmic-ray events, producing an observed peak in the sky map is then given by the expected statistical distribution of the total photon density at that location on the sky map. The expected statistical distributions, which are typically not Gaussian in shape, can be calculated directly from the PSF characteristics of the detector and placed into a lookup table to enable very fast searches for unknown gamma-ray sources. This technique is similar to maximum likelihood analyses in sensitivity but is computationally fast enough to perform a real-time transient search in a high data-rate detector like Milagro.

The 40 s–3 hr transient search is performed by first dividing the data into 20 s intervals and creating sky maps, both for the actual data ("on source") and for the expected background in each time interval. From these initial maps, 40 s sky maps are formed by summing all pairs of successive 20 s maps. The resulting set of sky maps is temporally oversampled by a factor of 2, with every 20 s map used twice so that a 40 s burst is guaranteed to be largely contained in one of the overlapping 40 s maps. A search is performed on each of these maps for emission using the test statistic described below, then pairs of the 40 s maps are combined to make 80 s maps (one-half of the 40 s maps are discarded to maintain the factor of 2 oversampling), and so on. The nine specific timescales that were searched are 40, 80, 160, 320, 640, 1280, 2560, 5120, and 10,240 s. The total observation days for each timescale are shown in the second column of Table 1. The longer timescales have slightly less observation time owing to gaps from occasional data dropouts. Full details of the transient search can be found in Morales (2002).

The significance of excesses in the on-source sky maps, compared to the background sky maps, is evaluated using a test statistic. The test statistic is very closely related to the probability of an observation being produced by a background fluctuation, with approximations used to speed up the analysis breaking the exact one-to-one relationship and leading to a slight flattening of the test statistic distributions (Morales et al. 2004). Since the value of the test statistic decreases with increasing transient flux (lower probability of the observation being produced by a back-
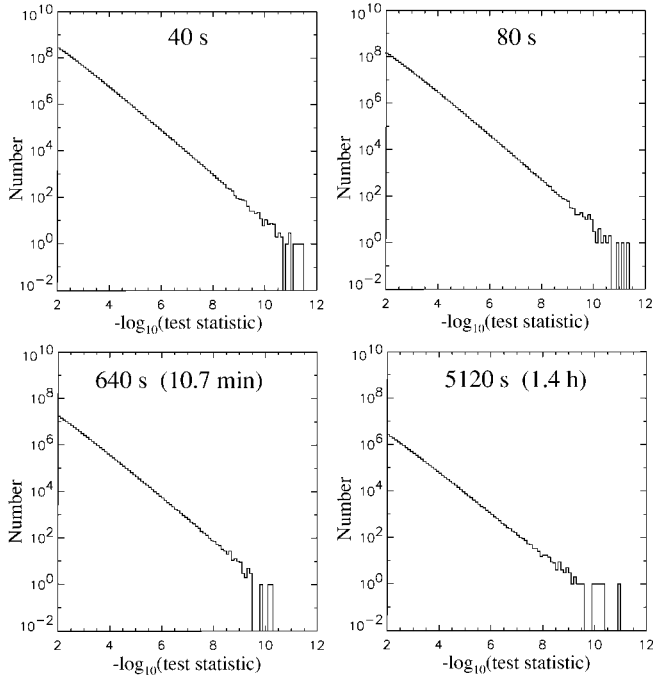
Fig. 1.—Test statistic distributions observed by Milagro between 2001 May 2 and 2002 May 22 for four representative timescales. No evidence for transient VHE emission was observed. No test statistic below 10^{-12} was observed in any of the nine timescales studied.
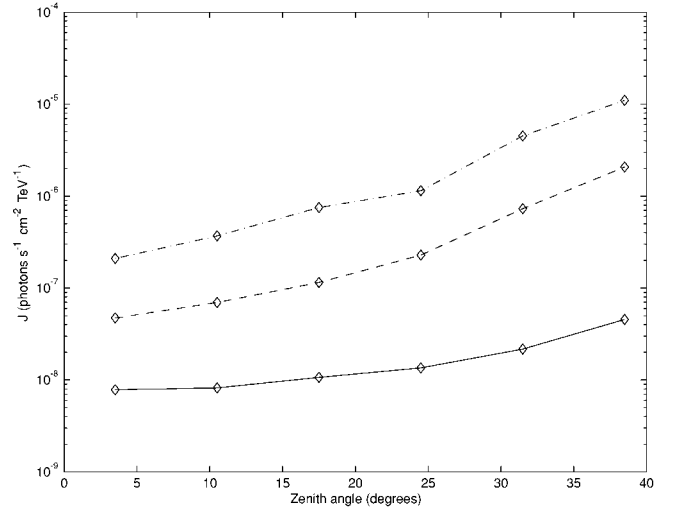

Fig. 2.—The 90% confidence upper limits for VHE transients of 40 s duration and an $E^{-2.0}$ spectrum for three different values of a hard spectral cutoff. The diamonds indicate the calculated limits on the normalization factor J in units of photons s^{-1} cm^{-2} TeV^{-1} for the spectrum $dN/dE = J(E/1 \text{ TeV})^{-2.0}$. Lines connecting the points have been drawn to guide the eye, with a solid line for a 21 TeV cutoff, dashed line for 1 TeV, and dash-dotted line for 300 GeV. Sensitivity values for the eight longer timescales (80, 160, 320, 640, 1280, 2560, 5120, and 10,240 s) are not plotted, but the sensitivity improves as a $J \propto t^{-0.64}$ power law with the duration of the VHE transient. Monte Carlo statistics lead to an uncertainty in the upper limits of 19%. Systematic errors are due principally to uncertainties in the Monte Carlo simulation and are estimated to be +40%/−20%, for a total estimated error of +44%/−27%.

ground fluctuation), a discovery search simply looks for values of the test statistic below that expected from the number of independent observations. If a transient is identified, the statistical significance can be calculated from the test statistic.

The data used for this analysis were taken between 2001 May 2 and 2002 May 22. Example distributions of the test statistic for four timescales are shown in Figure 1, with no observed location for any of the nine search intervals having a test statistic below the $\sim 10^{-12}$ value expected from the number of independent observations. There is no evidence for transient VHE emission of 40 s–3 hr duration in the Milagro data between 2001 May 2 and 2002 May 22.

3. LIMITS ON VHE GRB EMISSION

Two sets of constraints are presented here—upper limits on the VHE flux at the Earth and sensitivity distributions that constrain the absolute VHE luminosity of GRBs. The flux limits have the advantage of being independent of cosmological models and directly comparable to previous VHE GRB limits. However, because of the energy-dependent absorption of VHE photons by extragalactic background light (EBL), it is difficult to compare flux limits at the Earth to theoretical calculations. The sensitivity distributions place the observations into a theoretical context by correcting for absorption and cosmological effects. In conjunction with model predictions, these can be used to determine the maximum VHE luminosity at the source which is consistent with the observations presented in this Letter.

Since no observation in any of the nine timescales had a test statistic below 10^{-12}, we can use this as a threshold to set a conservative limit on the maximum flux consistent with these observations. The relationship between the gamma-ray flux and the test statistic was determined using a combination of Monte Carlo–generated transient VHE signals and real data background. The simulated detector signal was modeled from 100 GeV to

21 TeV as a function of zenith angle and observed spectrum, propagated through the Milagro reconstruction code, added to representative data, and fed to the 40 s–3 hr transient detection program. If the test statistic for the simulated signal fell below the 10^{-12} threshold of this study, the signal would have been stronger than any observed fluctuation on any timescale.

The flux limits represent the VHE transient signals that would have produced a signal with a test statistic below 10^{-12} 90% of the time (signal from a single burst that is excluded at the 90% confidence level). For this Letter, $E^{-2.0}$ power-law spectra extending from 100 GeV to hard spectral cutoffs at 300 GeV, 1 TeV, or 21 TeV (as observed local to the Earth) were chosen. These spectra serve as approximate models for an inverse Compton spectral bump at TeV energies or a hard VHE extension of the observed GRB spectrum past the multi-GeV observations of EGRET (Dingus 1995), with the spectral cutoff approximating either an intrinsic cutoff for nearby sources or EBL absorption for more distant sources. The limits are presented in Figure 2 as flux density as a function of zenith angle and burst duration.[15] Given the ~ 0.8 yr of observation time and the ~ 2 sr field of view, these flux limits provide the strongest constraints to date on the number of nearby bursts that emit TeV photons. For example, at a redshift of 0.024 (the 100 Mpc distance of the nearby bursts identified by Norris 2002, with the cosmology used in that paper), our 90% confidence limit for a spectrum that extends to 21 TeV and burst emission that lasts 40 s at a 10°.5 zenith angle is 1.1×10^{46} ergs s^{-1}.

However, at larger distances the usefulness of the limits from Figure 2 is complicated by the absorption of VHE photons by extragalactic background light (Jelley 1966; Primack et al. 1999; Stecker & de Jager 1998). The observed spectrum is a

---

[15] The full set of limits for $E^{-2.0}$ and $E^{-2.4}$ spectra without cutoffs are shown in Morales (2002).

convolution of the emitted spectrum and the extragalactic background light absorption—neither of which is well determined. Limits on the absolute VHE luminosity of GRBs are thus necessarily model dependent. In setting the limits that follow, Milagro is more sensitive than might initially be expected because bursts above $\sim 10^{51}$ ergs s^{-1} are sufficiently bright to be detected even after extinction of a few optical depths.

In an effort to place the current observations in context, a set of assumptions about the emitted spectrum, EBL absorption, and cosmology has been chosen and sensitivity distributions calculated within this theoretical framework. For a set of source luminosities and durations, simulated GRBs were created with an $E^{-2.0}$ emission spectrum from 100 GeV to 21 TeV, an isotropic sky position, and following the star formation rate (SFR) in z. The EBL absorption was determined by J. R. Bullock, R. S. Somerville, & J. R. Primack (2004, in preparation; similar to Primack et al. 1999) using recent results from semianalytic modeling and includes collisional starburst effects and a Kennicutt initial mass function (Kennicutt 1983).[16] A ΛCDM cosmology ($\Omega_M = 0.3$, $\Omega_\Lambda = 0.7$, $h = 0.65$) was used for both the EBL calculation and the cosmological corrections. The results are rather insensitive to the emitted spectrum and cutoff energy owing to the strong EBL absorption, which eliminates nearly all emission above 300 GeV at redshift ≈ 0.3 and limits the distance to which Milagro can observe VHE emission to redshift $\lesssim 0.7$. The SFR was modeled as $10^{1.45z-1.52}$ $M_\odot$ Mpc^{-3} yr^{-1} for $z < 0.9$ and 0.61 $M_\odot$ Mpc^{-3} yr^{-1} for $z \geq 0.9$ within each redshift bin, following the discussion in Hopkins et al. (2001).

The results of the sensitivity calculation are presented in Table 1 as the probability that Milagro would have observed a VHE GRB (i.e., test statistic $<10^{-12}$) as a function of the absolute luminosity,[17] distance, and duration of the source. Owing to increased atmospheric depth away from detector zenith, the low-energy threshold of Milagro increases with zenith angle, as can be seen in Figure 2 by the decreased sensitivity at large zenith angles when the emission is limited to lower energies. As GRBs become increasingly distant, the EBL absorption effectively truncates the observed spectrum above a few hundred GeV. These effects lead to the effective field of view of Milagro becoming narrower with increased redshift, producing the gradual decline in detection probability seen in Table 1.

Given theoretical expectations for the GRB distance, luminosity, and duration distributions, the probabilities in Table 1

can be used to calculate the upper limits provided by these observations. For a 90% confidence upper limit, the maximum GRB rate consistent with these observations is given by multiplying the expected number of GRBs within each redshift bin by the detection probability in Table 1 and adjusting the total number of GRBs until the mean number of events seen by Milagro is 2.3. If the model GRB distance distribution does not follow the SFR, the probabilities in Table 1 can still be used as approximate values, or corrections can be applied to adjust for the distribution of events within each bin. The results are typically quoted as the number of GRBs $M_\odot^{-1}$ of star formation or the average number of GRBs Gpc^{-3} yr^{-1}.

As an example, consider a model that predicts that GRBs follow the SFR, with all GRBs emitting a characteristic 80 s pulse of VHE emission. The resulting 90% confidence upper limits for this model are 6.2×10^{-8} GRBs $M_\odot^{-1}$ of star formation (an average of 4.8 GRBs Gpc^{-3} yr^{-1} over $0 < z < 0.5$) for an isotropic luminosity of 10^{51} ergs s^{-1}, or 1.1×10^{-8} GRBs $M_\odot^{-1}$ of star formation (an average of 0.8 GRBs Gpc^{-3} yr^{-1} over $0 < z < 0.5$) for a luminosity of 10^{52} ergs s^{-1}, with significantly tighter constraints if the GRB distribution trails the SFR (i.e., there are more low-redshift GRBs). Of the 36 GRBs with known distances, five have a redshift below 0.5.[18] If the GRBs detected by BATSE follow the same distance distribution, a rough estimate of the observed GRB rate yields ~ 2.6 GRBs Gpc^{-3} yr^{-1}, or $\sim 3.4 \times 10^{-8}$ GRBs $M_\odot^{-1}$ of star formation if they follow the SFR. While detailed model calculations are needed to convert the probabilities in Table 1 into meaningful upper limits, comparison with the limits from this simple model suggests that if GRBs follow the SFR, the typical luminosity of 40 s–3 hr VHE GRB counterparts is constrained to be similar to or less than the prompt keV–MeV emission.

---

[16] The magnitude of the EBL absorption is quite uncertain, and the models by Stecker & de Jager (1998) have considerably less attenuation. Consequently, the limits presented here may be conservative.

[17] The luminosity quoted is the isotropic luminosity assuming no beaming at the source and is used to facilitate comparison with MeV–GeV measurements.

[18] One can use this fraction to roughly estimate that if all bursts were 10^{51} ergs s^{-1}, they would yield a flux brighter than the sensitivity in Fig. 2 ($\sim 10^{-7}$ cm^{-2} s^{-1}) out to a redshift of about 0.5 for zenith angles less than $\sim 30°$, and approximately $(5/36)0.84/4\pi = 1\%$ of all bursts would be detectable by Milagro.

REFERENCES

Amenomori, M., et al. 1996, A&A, 311, 919
Atkins, R., et al. 2000a, ApJ, 533, L119
———. 2000b, Nucl. Instrum. Methods Phys. Res., 449, 478
———. 2003, ApJ, 595, 803
Connaughton, V., et al. 1997, ApJ, 479, 859
———. 1998, Astropart. Phys., 8, 179
Dermer, C. D., & Chiang, J. 2000, ApJ, 537, 785
Dingus, B. L. 1995, Ap&SS, 231, 187
Gonzalez, M. M., Dingus, B. L., Kaneko, Y., Preece, R. D., Dermer, C. D., & Briggs, M. S. 2003, Nature, 424, 749
Hopkins, A. M., Connolly, A. J., Haarsma, D. B., & Cram, L. E. 2001, AJ, 122, 288
Jelley, J. V. 1966, Phys. Rev. Lett., 16, 479

Kennicutt, R. C., Jr. 1983, ApJ, 272, 54
Leonor, M. I. R. 2000, Ph.D. thesis, Univ. California, Irvine
McCullough, J. F. 2001, Ph.D. thesis, Univ. California, Santa Cruz
Morales, M. F. 2002, Ph.D. thesis, Univ. California, Santa Cruz
Morales, M. F., Williams, D. A., & DeYoung, T. 2004, Astropart. Phys., 20, 485
Norris, J. P. 2002, ApJ, 579, 386
Padilla, L., et al. 1998, A&A, 337, 43
Pilla, R. P., & Loeb, A. 1998, ApJ, 494, L167
Primack, J. R., Bullock, J. S., Somerville, R. S., & MacMinn, D. 1999, Astropart. Phys., 11, 93
Stecker, F. W., & de Jager, O. C. 1998, A&A, 334, L85
Zhang, B., & Mészáros, P. 2001, ApJ, 559, 110